OPTIMIZATION AND APPLICATION OF TEMPERATURE FIELD IN RAPID HEAT CYCLING MOLDING

by

Mingliang HAO[a] and Haimei LI[a,b*]

[a] School of Materials Science and Engineering, Zhengzhou University, Zhengzhou, Henan
[b] Jiangsu Huililong Plastic Group Co. Ltd, Suining, Jiangsu, China

Original scientific paper
https://doi.org/10.2298/TSCI210606291H

The rapid thermal cycle molding belongs to the injection mold temperature control system which is helpful to improve moldability and enhance part quality. Despite many available literatures, rapid thermal cycle molding does not represent a well-developed area of practice. The challenge is the uneven distribution of temperature in the cavity after heating, which mostly leads to defects on the surface of the products. In order to obtain uniform cavity surface temperature distribution of rapid thermal cycle molding, the power of heating rods of the electric-heating system in an injection mold was optimized by the response surface method in this work. The proposed optimization result was applied to design a complex rapid thermal cycle molding injection mold with side core-pulling, holes, and different thickness of an automotive part to verify its effectiveness by injection molding. Compared with initial design, the mold temperature uniformity was remarkably improved by 79%. Based on the optimization and injection molding numerical simulation results, the workable molding process to weaken the weld-lines effects on the quality was suggested and the practical injection molded parts were well produced.

Key words: *rapid thermal cycle molding, optimization design of heating rod, response surface method, injection molding, numerical simulation*

Introduction

The injection molding is ideally suited to fabricate mass-produced parts with complex shapes and precise dimensions, so it is widely used in household appliances, automobils, communications and other fields. In conventional injection molding (CIM), the mold temperature raises mainly depends on multi-cycle injection, and the mold temperature does not change significantly in the whole cycle, almost a constant, that not only wastes a lot of raw materials but also causes lower efficiency. Also, the CIM process with invariable mold temperature control, usually suffers from issues caused by the big temperature difference in the mold and the polymer melt [1]. To reduce inhomogeneity of the products properties, it is key that filling with high temperature and cooling with low temperature during a production cycle. Several techniques based on temperature control have been suggested to improve the quality of molded parts, mainly named rapid heating cycle molding (RHCM) technologies [2-10], such as flame heating [2], hot liquid medium (water and oil) heating [3], steam heating [4], infrared heating [5], induction heating [6, 7], electric heating rod [8] and so on. The RHCM

* Corresponding author, e-mail: haimeili@zzue.edu.cn

is a technology keeping high mold temperature during filling while lowering the mold temperature to below a certain value during the post-filling/cooling without a large increase in production cycle and energy consumption. Before melt injection, the mold cavity surface was rapidly heated up to the polymer-softening temperature. During filling and packing, the elevated mold temperature is maintained until the cooling stage begins. The polymer melt in mold cavity is quickly solidified by fast cooling of the metal mold. Then the parts are ejected and one RHCM cycle is over. Through this dynamic rapid mold cavity temperature control method, RHCM process is able to maximize part quality with minimal effects on processing cycle time. The temperature uniformity, efficiency of energy, and maximum available heating power are often used to evaluate the performance of RHCM. The uniformity and heating efficiency have direct influence on processing quality and molding cycle time. Therefore, many researchers used numerical optimization algorithms to improve the temperature uniformity [10-15] and heating efficiency [5, 6].

Quantitative evaluation of RHCM by means of analytical and numerical methods is regarded as an important means to optimize and design a capable mold temperature control system [1, 8-13]. Xiao and Huang [1] applied particle swarm optimization and finite element method (FEM) to optimize an electric-heating system for a blow molding of an automotive spoiler, and the surface quality of products was dramatically improved. Vallejo *et al.* [11] used the response surface method (RSM) to optimize heating system and obtained uniform temperature of cavity surface. Li *et al.* [12] optimized the heating rods by response surface and genetic algorithm. However, it is not easy to implement the RHCM technology because of the diversity and complexity of the injection mold which is involving different materials for insulation and heating. In this paper, we applied the RHCM technology based on thermal simulation and alternatively a coupled heat and flow analysis to a complex mold with side core-pulling holes and different thicknesses, in which the automobile spare parts were produced. Box-Behnken experimental design (BBD) and RSM were used to optimize the RHCM system and obtain the ideal temperature distribution of mold cavity. Then optimization results of RHCM system were used as the input data of injection molding simulation. Finally, the weld lines or melt lines caused by injection mold structure of an automobile spare part were improved, and the feasibility of optimal RHCM was verified.

The RHCM mold design of an automobile spare part

Injection mold structure

The injection mold with RHCM system is composed of different parts, fig. 1. The cavity/core is an insert and the length, width and height dimensions are 100 mm, 100 mm, and 45 mm respectively. Heating and cooling lines have their own independent mold plates, figs. 1(b)-1(d). As for the complicated structure with insert, holes and different thicknesses, we resembled the principle of efficiency and cost of the factory and applied them to design heating lines, cooling lines and heating manners [2, 5, 16, 17]. The heat lines, fig. 1(c), with the same diameter, D = 6 mm, were arranged along horizontal interval about 10 mm and profile almost conformal the mold cavity. The general rule of thumb is that the distance between heating lines is 1.5-2 D, and the distance between heating rods and cavity surfaces is 1-1.5 D. Similarly, the cooling lines dimensions and layout were arranged, fig. 1(d). The challenge of this RHCM system lies in the parting surface of injection mold is not in a plane. The mold and polymer properties for simulations are listed in tab. 1.

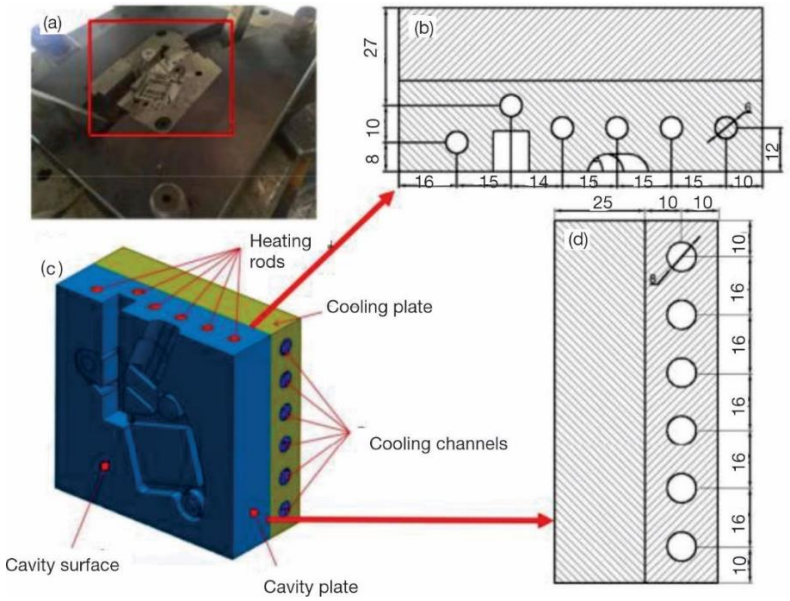

Figure 1. Schematics of mold structures and dimensions; (a) the real mold, (b) the digital model of RHCM mold with multi-layer, (c) the locations and dimensions of electric heating rods, and (d) the locations and dimensions of cooling channels

Table 1. The properties of mold materials and polymer

Name	Material	Density [kgm^{-3}]	Thermal conductivity [Wm^{-1}K^{-1}]	Capacity [Jkg^{-1}K^{-1}]
Cavity plate	AISI P20	7850	34	460
Cooling plate	Aluminum	2700	210	900
Stationary mold plate	HT350	7800	47	440
Polyoxymethylene (POM)	POM melt	1.140	0.224	2160
	POM solid	1.424	0.260	1740

Thermal analysis

The RHCM system is mainly used to help the polymer melt fill cavity, keep the polymer from cooling and avoid the potential processing defects. There are two mechanisms related to mold rapid heating. One is heat generation source and the other is heat conduction that takes effect through appropriate boundary conditions [2]. Among all possible heat sources, electrical rod heating is the most widely used [2, 14-22]. The heat transfer process of the entire RHCM system is a 3-D transient heat conduction problem with an internal heat source. The governing equation was described [9, 10]:

$$\frac{\partial}{\partial x}\left(k\frac{\partial T}{\partial x}\right)+\frac{\partial}{\partial y}\left(k\frac{\partial T}{\partial y}\right)+\frac{\partial}{\partial z}\left(k\frac{\partial T}{\partial z}\right)+\dot{q}=\rho c_p\frac{\partial T}{\partial t} \tag{1}$$

where k [Wm^{-1}K^{-1}] is the heat conductivity, $\dot{q}$ [Wm^{-3}] – the internal heat source, ρ [kgm^{-3}] – the materials density, c_p [Jkg^{-1}K^{-1}] – the materials specific heat.

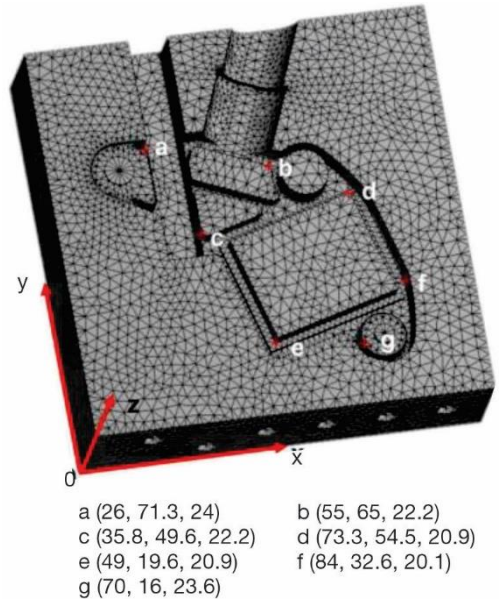

Figure 2. The 3-D mesh model of mold for FEM simulation and the selected special locations to investigate temperature uniformity

Reasonable simplifications and assumptions were made based on the practical processing. First, the thermal properties of different mold materials were regarded as constants. Then, the contact thermal resistance between different mold plates was neglected, including interface of the heating rods and heating channels. Subsequently, the heat contribution of each heating rod was treated as heat flux and estimated (2) [11]:

$$\dot{q} = \frac{P}{\pi DL} \tag{2}$$

where P is the power of the heating rod, π – the circular constant, D and L – the diameter and length of heating rods, respectively.

To understand the heat transfer process within a whole RHCM process, the numerical analysis of the initial RHCM were constructed by finite element analysis (FEA). The FEA meshes are shown in figs. 2 and 3. The selected seven special locations at different planes of the complex cavity were used to investigate the temperature uniformity, fig. 2. The initial and boundary conditions [2, 22, 23] of FEA simulation are shown in fig. 3. The polymer was POM (LG Chemical, Korea) and its thermal deformation temperature is about 100 °C. The temperature of mold cavity surface was set to 100 °C according to the industrial requirements. The initial temperature of mold cavity plates was equal to the ambient temperature of 30 °C. The continued heating time was set as 30 seconds.

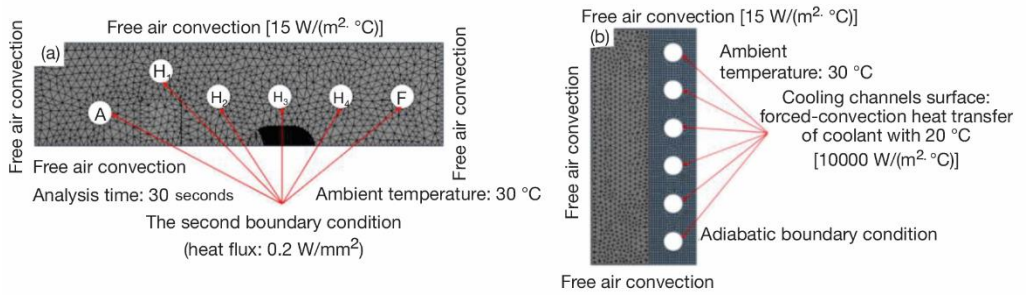

Figure 3. The 3-D mesh models and boundary conditions of heating and cooling analysis; (a) mold plate with heating channels and (b) mold plate with cooling lines

Heating temperature field of initial design

To investigate the initial design of RHCM, we focused on the mold surface temperature difference of the special locations during whole heating stage. The numerical results of original RHCM heating stage are shown in fig. 4. The cavity surface temperature rises with time until the heating end, t_h = 30 seconds. Also the temperature difference between selected

points increases with time simultaneously, fig. 4(a). The heating rates of different points of cavity surface are similar, all at the range of 4.5-5 °C per second. The time for required mold temperature is in the range of 19-24 seconds. The maximum temperature difference is between point "a" and point "b", or point "a" and point "f", dash line in fig. 4(a).

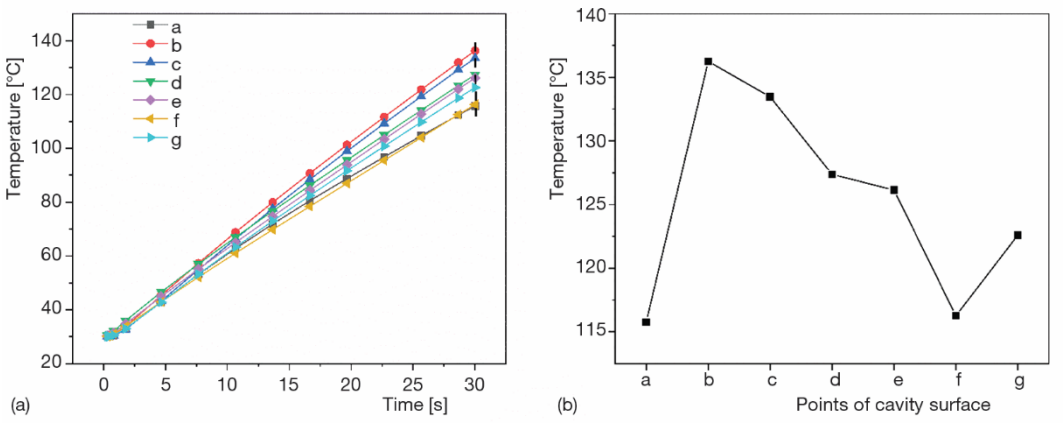

Figure 4. Temperature results of selected points at initial design mold surface during heating stage; (a) temperature variations with time and (b) temperature distribution at the end of heating

The temperature at point "a" is the lowest because the distance between "a" and the corresponding heating rod line is the largest. Thus, there is less heat conduction and heat radiation compared with others. Accordingly the temperature at point "b" is the highest, because point "b" is in the middle location of mold plate, right above the corresponding heating rod with the shortest heat transfer distance. According to the initial analysis results, the distribution of temperature field after heating 30 seconds is uneven, and the maximum temperature difference of cavity surface reaches 21 °C, which obviously cannot meet the processing requirements. Although rapid heating rods system (mold plates, number of heating lines, the heating lines layout, *etc.*) was carefully considered based on the design rules described in references [4, 12-14], it was difficult to obtain even cavity surface temperature because of the complicated cavity structure. The automobile injection molded parts, fig. 1, is relatively small and the narrow space confined the change of heating rod location and dimension size. Therefore, the only adjustment parameter is the power density of each heating rod.

Optimization of heating rods by RSM

Optimization model

From the numerical results of initial temperature field, fig. 3, and mold structure, fig. 2, we know that mold surface temperatures of point 'a' and point 'f' are low. Therefore the power densities of heating rod "A" and "F" correspond to mold surface point "a" and "f" need to set a higher values, and their power densities are set as 0.27 W/mm^2 and 0.25 W/mm^2, respectively. The power densities of heating rod H_1, H_2, H_3, and H_4 were considered as the design variables. Based on accumulated experiences [1, 11, 12, 20] and engineering analysis, 0.18 W/mm^2, 0.22 W/mm^2 were the lower and upper boundary of the design variables respectively. Therefore, the optimization problem was built [12, 20]:

$$\begin{gathered} \textit{Find } H_i, \quad i = 1,2,3,4 \\ \min_{k\in R} \Delta T_k = \min_{k\in R}\{\max(T_k - T_{k+1})\} \\ \textit{subject } \Delta T \le 5\ ^\circ\mathrm{C} \\ \textit{Within the range}: 0.18 \le H_i \le 0.22 \end{gathered} \tag{3}$$

where H_i (i = 1, 2, 3, 4) is the design variable, representing the power of the four heating rods and T_k – the temperature of the special point k during the heating process, k = 1, 2, … , n. In this study, n is 7. The R is the set of the tracking points, here is the set of points 'a', 'b', 'c', 'd', 'e', 'f', and 'g'. The variation of H_i causes the change of T_k. Therefore, T_k is the function of the design variable H_i.

Optimization process

Understanding the relationship between the maximum mold temperature difference and the power densities of the heating rods is helpful to optimize the surface temperature field of the mold. The RSM is a method of approximating implicit limit state functions by polynomial functions through a series of deterministic experiments. Here, RSM [6, 20] was applied to specify the effects of each heating rod power density on cavity surface temperature of the RHCM. The mathematical model of the expected responses for optimization was built through numerical experiment design and regression analysis [12, 24]:

$$Y = \beta_0 + \sum_{i=1}^{m}\beta_i x_i + \sum_{i=1}^{m}\beta_{ii} x_{ii} + \sum_{i=1}^{m-1} x_1 \sum_{j=1}^{m}\beta_{ij} x_j + \varepsilon \tag{4}$$

where β_0 is the constant, β_i, β_{ii}, β_{ij} denotes the coefficient of each item, m represents the number of variables, and ε means the statistical error. In this work, m is 4, *i.e.* the number of heating rods. The Y means the response variable, *i.e.* the temperature difference of mold surface. A series of experiments should be done to obtain the specific values relevant to response variable Y. There, the BBD [6, 11] were applied to evaluate the design parameters effects on response variables. According to rules of BBD and the consideration of accuracy, 29 experiment samples were arranged, tab. 2.

In order to obtain the cavity surface temperature distribution (response values) under different heating rods power, numerical experiments were carried out. The transient heat analysis was carried out by ANSYS, and the analysis conditions were all set the same as the initial design discussed above except for the different heating rods power. The maximum temperature difference on the cavity surface under different conditions was obtained and shown in the last column of tab. 2.

Analysis of variance (ANOVA) was used to test the significance of the mathematical model [6], and the results of analysis of variance are shown in tab. 3. The value of *sum of squares* shows in the second column of tab. 3 represents the sum of squares of each item. The degrees of freedom (DoF) represent the number of estimated parameters used to compute the sum of squares of source. The F-value of 11.01 implies the model term is significant. The P-value (probability) is mainly used to test the significance of the model item. When the P-value is less than 0.05, the model item is considered significant. In the table, A, B, D, C^2, D^2, which are matching H_1, H_2, H_4, H_3^2, and H_4^2, are significant terms. On the contrary, when the p-value of a certain model item is greater than 0.1, it indicates that the item has little influence on the

Table 2. Box-Behnken experiment design and numerical results

Experiment no.	Design variable				Response
	H_1 [Wmm^{-2}]	H_2 [Wmm^{-2}]	H_3 [Wmm^{-2}]	H_4 [Wmm^{-2}]	$\triangle T_{max}$ [°C]
1	0.2	0.22	0.2	0.18	18.42
2	0.22	0.22	0.2	0.2	17.61
3	0.2	0.2	0.18	0.18	14.65
4	0.22	0.2	0.2	0.22	10.43
5	0.2	0.2	0.2	0.2	10.23
6	0.2	0.22	0.2	0.22	12.6
7	0.2	0.2	0.22	0.18	14.64
8	0.2	0.18	0.2	0.18	12.44
9	0.2	0.2	0.2	0.2	10.23
10	0.22	0.18	0.2	0.2	11.1
11	0.22	0.2	0.2	0.18	16.55
12	0.2	0.22	0.22	0.2	16.67
13	0.18	0.2	0.2	0.22	7.15
14	0.2	0.2	0.2	0.2	10.23
15	0.18	0.2	0.2	0.18	11.99
16	0.18	0.22	0.2	0.2	12.58
17	0.18	0.2	0.18	0.2	8.22
18	0.18	0.18	0.2	0.2	6.14
19	0.2	0.2	0.2	0.2	10.23
20	0.2	0.18	0.18	0.2	10.17
21	0.2	0.18	0.2	0.22	5.02
22	0.2	0.22	0.18	0.2	15.07
23	0.22	0.2	0.22	0.2	14.01
24	0.2	0.2	0.22	0.22	11.25
25	0.18	0.2	0.22	0.2	11.76
26	0.2	0.2	0.18	0.22	14.64
27	0.2	0.2	0.2	0.2	10.23
28	0.22	0.2	0.18	0.2	13.2
29	0.2	0.18	0.22	0.2	9.11

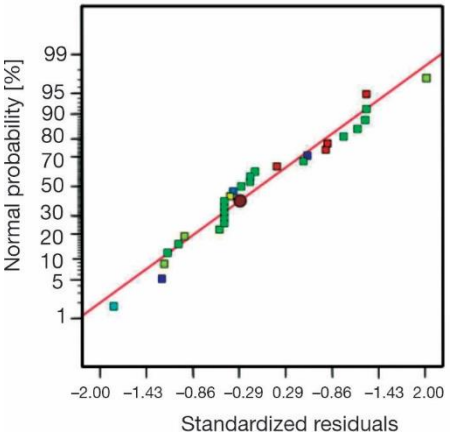

Figure 5. The normal probability distribution diagram of the residual of the ΔT_{max} (maximum temperature difference on the surface of the cavity)

response value of the design space. Therefore, we can reduce the quadratic term with less contribution to response value in eq. (4). Meanwhile, it is shown in fig. 5 that the residual error of each response variable almost falls on a straight line, which shows that the error is normally distributed, and proves that these mathematical models are adequately fitted by the least squares regression technique. [6, 11, 12]. Consequently, the response surface regression equation was developed:

$$\Delta T_{max} = 248.6959 + 104.416H_1 + 162.375H_2 - \\ -1566.7178H_3 - 1236.676H_4 + \\ +3932.3153H_3^2 + 2804.1903H_4^2 \quad (5)$$

Table 3. The ANOVA results for the maximum mold surface temperature difference

Source	Sum of squares	DoF	Mean square	*F*-value	*P*-value	
Model	278.70	14	19.91	11.01	< 0.0001	significant
A-H_1	52.33	1	52.33	28.94	< 0.0001	
B-H_2	126.56	1	126.56	69.98	< 0.0001	
C-H_3	0.19	1	0.19	0.10	0.7538	
D-H_4	63.48	1	63.48	35.10	< 0.0001	
AB	0.0012	1	0.0012	0.0007	0.9796	
AC	1.86	1	1.86	1.03	0.3273	
AD	0.41	1	0.41	0.2265	0.6415	
BC	1.77	1	1.77	0.98	0.3395	
BD	0.64	1	0.64	0.35	0.5614	
CD	2.86	1	2.86	1.58	0.2294	
A^2	0.18	1	0.18	0.10	0.7546	
B^2	5.76	1	5.76	3.18	0.0961	
C^2	19.86	1	19.86	10.98	0.0051	
D^2	10.93	1	10.93	6.05	0.0276	
Residual	25.32	14	1.81			
Total	304.02	28				

Optimization results and confirmation

Through the previous verification analysis, tab. 3 and fig. 5, it is found that the obtained mathematical model, eq. (5), is well describe the relationship between response quantity

and design variables. Therefore, we use it conveniently to optimize the temperature field distribution on the cavity surface. According to the corresponding equation, when Y is minimal, H_1 = 0.18 W/mm², H_2 = 0.18 W/mm², H_3 = 0. 2 W/mm², H_4 = 0.22 W/mm². In this case, through the simulation experiment, the maximum temperature difference of the cavity surface is 4.39 °C. Compared to the maximum temperature difference of initial design (21 °C, shown in fig. 4), the difference is reduced by 79.1%, fig. 6(b). It is proved that the optimum design of heat rod power by RSM is valid. Comparison of temperature field before and after optimization is shown in fig. 6.

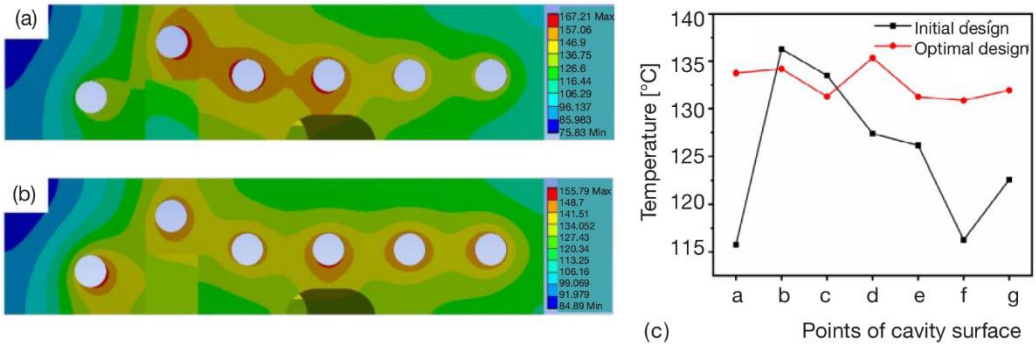

Figure 6. Temperature results of RHCM before and after optimization; (a) the temperature distribution of initial design, (b) temperature distribution of optimization, and (c) the selected points temperature before and after optimization

As the cooling start-up, the heating rod was shut down and the coolant begun to circulate in cooling lines [25]. The cooling temperature field distribution before and after optimizing the power densities of heating rods is shown in fig. 7. Although absolute value of the maximum temperature difference between the mold surface locations before and after optimization is similar, the optimized cavity temperature distribution is more uniform locally (the corresponding locations at different planes in red and blue ellipses shown in fig. 7).

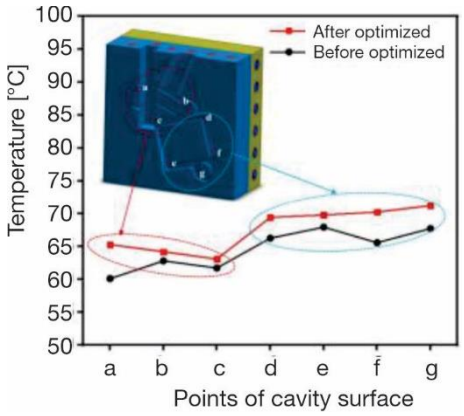

Figure 7. The selected points temperature results of cooling before and after optimization

Engineering application of RHCM

To demonstrate the benefits of a high and uniform cavity surface temperature, the weld line or melt line issue here was investigated carefully by Moldflow Insight (Auto Desk Inc., USA). Here we assumed that the uniformity of temperature is an ideal state *i.e.* the temperature is almost same after optimum. The parameters of injection molding are listed in tab. 4. The simulated filling and weld line results are shown in figs. 8 and 9 respectively. The melt filling of RHCM (100 °C) is faster than that of CIM (50 °C), fig. 8, but the filling pattern are similar. It is shown that the flow fronts separated and rejoined again during filling. Weld lines and/or melt lines are formed, fig. 9. There are three different types weld lines by formation show in fig. 9(c). First L1 is

Table 4. The parameters of injection molding simulation

Parameters	Values
Required mold temperature, [°C]	50/100
Melt temperature, [°C]	225
Filling rate, [cm^3s^{-1}]	17

caused by the through holes structure inevitably. Second L2 is caused by different thicknesses. Third L3 is caused by slide-core (deep hole). So the melt front merge angle (V-notch angle) [26] of L3 weld line/melt line was selected as an index to discuss the RHCM merits.

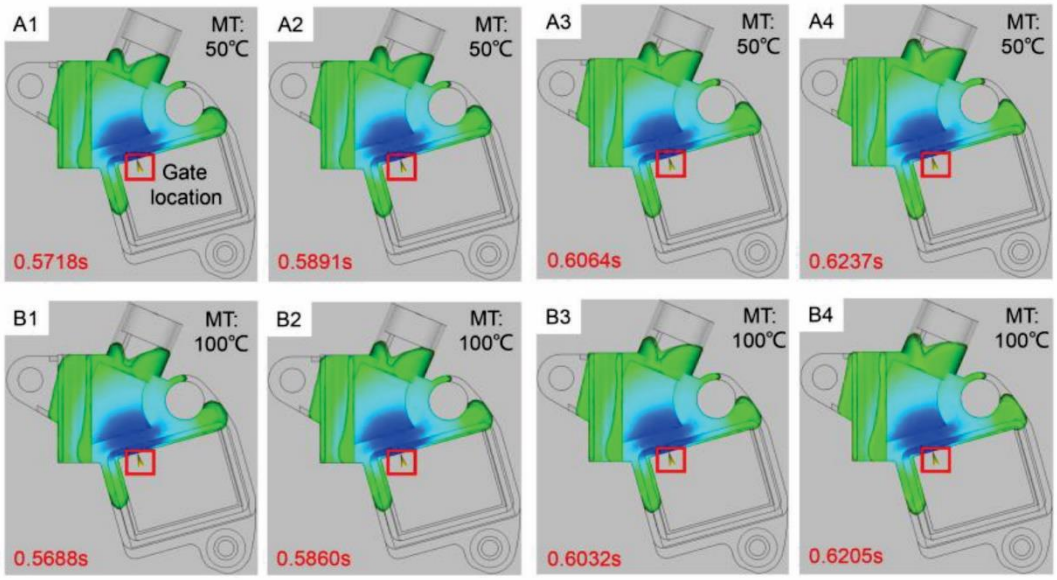

Figure 8. The comparison of melt flow front at different mold temperatures or processes, (A1-A4, 50 ℃ of CIM, B1-B4 100 ℃ of RHCM)

Although the weld lines of injection molded parts of both CIM and RHCM are obvious in naked eye, the quantification of melt front merge angle and melt temperature are different. As for the RHCM, the melt merge angle of selected points at L3 weld lines W1-W3, fig. 10(a), is larger (75-90°) than that of CIM (60-80°), which means better welding strength [27]. Since melt temperature is an important factor for weld line strength, we also compared the changes of melt temperature variation with time during filling, fig. 10(c). It is shown that higher mold temperature (RHCM) with higher melt temperature is benefit to divided melt fronts bonding better, which is consistent with the welding angle results [28].

Unfortunately, RHCM also have limit to improve all weld lines in this case. In the practical application of RHCM, appropriate modifications of mold structure are made based on numerical and optimization results under the current conditions. Firstly, metal inserts in the corresponding places were used to increase the strength weaken by weld line. Then, texture was applied to improve the surface quality. According to our suggestions and process optimization, the processed products are shown in the fig. 9(d). And the appearance and strength of the parts meet the industrial requirement.

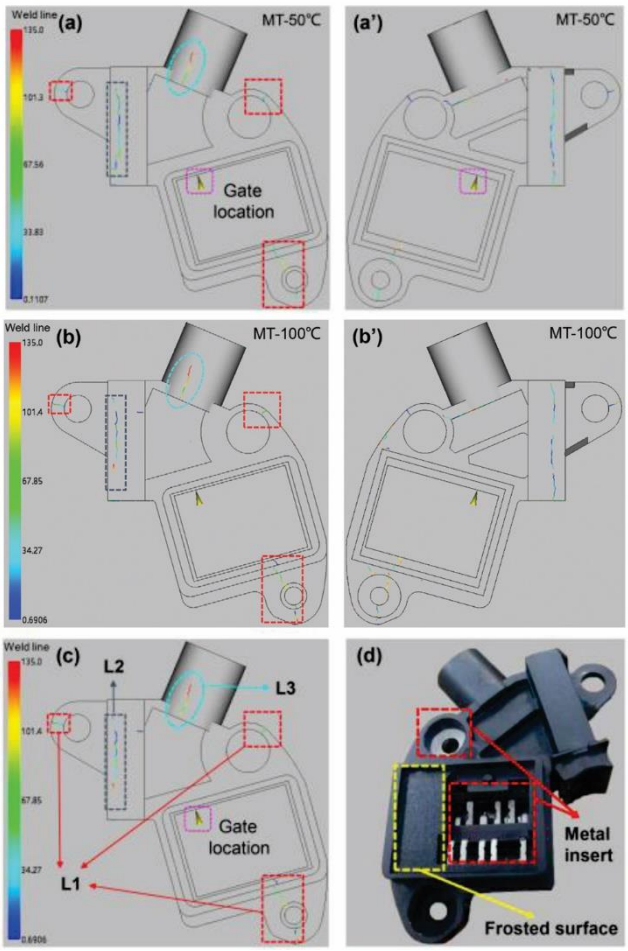

Figure 9. The weld lines/melt lines results of CIM, RHCM, and the real product; (a) the front results of CIM, (a') the back results of CIM, (b) the front results of RHCM, (b') the back results of RHCM, (c) selected locations labeling of weld lines/melt lines, and (d) a real product

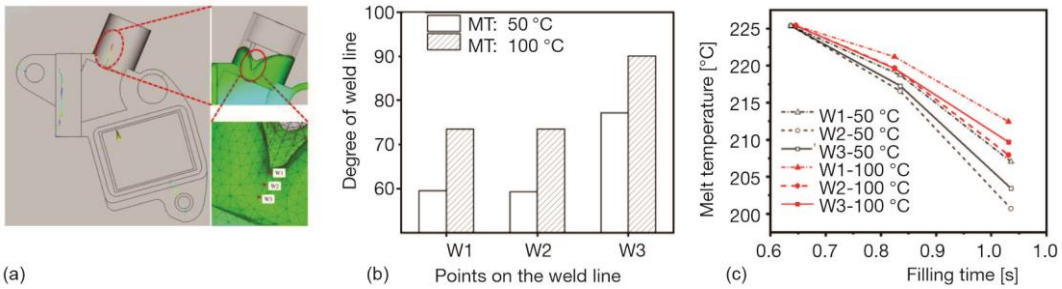

Figure 10. Quality comparison diagram of welding line at different mold temperatures; (a) the location of the pick-off point on the weld line, (b) the weld line angle comparison of CIM and RHCM, (c) the melt temperature at the same point during filling of different mold temperatures

Conclusions

We established the 3-D model of the rapid thermal cycle mold, and then simulated the temperature field distribution with ANSYS. To obtain even mold surface temperature, the optimization model of an injection mold with RHCM was done by the BBD and RSM. The optimal heater power combination shows that the temperature uniform distribution of the cavity surface is improved notably by 79%. The features of weld lines or melt lines of injection molded automotive parts by different processing were compared emphatically through numerical simulation. The results show that the welding merged angle is improvement obviously when the mold temperature is higher by RHCM.

Due to the complex cavity structure, the heating efficiency associated with production efficiency and the temperature uniformity associated with product quality are hard to optimize simultaneously.

In practical term there is a balance between the two factors. In the future work, we will further quantitatively investigate the relationships between RHCM, production efficiency and processing quality.

Nomenclature

c_p – specific heat [Jkg^{-1}K^{-1}]
D – diameter, [m]
H_i – number of the heating rods, [–]
L – length, [m]
k – heat conductivity, [Wm^{-1}K^{-1}]
P – power of the heating rods, [W]
$\dot{q}$ – internal heat source, [Wm^{-3}]
T – temperature, [°C]
t – time, [s]
t_h – heating time, [s]
ΔT_k – temperature difference, [°C]

Greek symbols

ρ – density, [kgm^{-3}]
β – coefficient, [–]
π – circular constant, [–]

Acknowledgment

This work was financially supported by project of "the Jiangsu Innovative and Entrepreneurial Talent".

References

[1] Xiao, C. L., Huang, H. X., Optimal Design of Heating System for Rapid Thermal Cycling Mold Using Particle Swarm Optimization and Finite Element Method, *Applied Thermal Engineering*, *64* (2014), 1-2, pp. 462-470
[2] Yao, D. G., *et al.*, Rapid Thermal Cycling of Injection Molds: An Overview on Technical Approaches and Applications, *Advances in Polymer Technology*, *27* (2008), 4, pp. 233-255
[3] Li, J. Q., *et al.*, An Experimental Study of Skin Layer in Rapid Heat Cycle Molding, *Polymer-Plastics Technology and Engineering*, *53* (2014), 5, pp. 488-496
[4] Saito, T., *et al.*, A New Concept of Active Temperature Control for an Injection Molding Process Using Infrared Radiation Heating, *Polymer Engineering and Science*, *42* (2002), 12, pp. 2418-2429
[5] Wang, G. L., *et al.*, Analysis of Thermal Cycling Efficiency and Optimal Design of Heating/Cooling Systems for Rapid Heat Cycle Injection Molding Process, *Materials & Design*, *31* (2010), 7, pp. 3426-3441
[6] Wang, G. L., *et al.*, Multi-objective optimization design of the heating/cooling channels of the steam-heating rapid thermal response mold using particle swarm optimization, *International Journal of Thermal Sciences*, *50* (2011), 5, pp. 790-802
[7] Zhao, G. Q., *et al.*, Research and Application of a New Rapid Heat Cycle Molding with Electric Heating and Coolant Cooling to Improve the Surface Quality of Large LCD TV Panels, *Polymers for Advanced Technologies*, *22* (2011), 5, pp. 476-487
[8] Chen, S. C., *et al.*, Dynamic Mold Surface Temperature Control Using Induction Heating and Its Effects on The Surface Appearance of Weld Line, *J. of Applied Polymer Science*, *101* (2006), 2, pp. 1174-1180
[9] Hua, C. H., Wang, K. J., Optimization of a 3-D High-Power LED Lamp Orthogonal Experiment Method and Experimental Verification, *Thermal science*, *25* (2021), 2B, pp. 1495-1500

[10] Chen, S. C., *et al.*, Simulations and Verifications of Induction Heating on a Mold Plate, *International Communications in Heat and Mass Transfer*, *31* (2004), 7, pp. 971-980
[11] Vallejo, F. J. C., *et al.*, Optimization of the Heating System by Electrical Resistances in a Rapid Thermal Response Mold Based on MSR-PSO-FEM, *Revista Internacional de Metodos Numericos para Calculo y Diseno en Ingenieria*, *35* (2019), 3, p. 40
[12] Li, X. P., *et al.*, Optimal Design of Heating Channels for Rapid Heating Cycle Injection Mold Based on Response Surface and Genetic Algorithm, *Materials & Design*, *30* (2009), 10, pp. 4317-4323
[13] Nian, S. C., *et al.*, Key Parameters and Optimal Design of a Single-Layered Induction Coil for External Rapid Mold Surface Heating, *Int. Communications in Heat and Mass Transfer*, *57* (2014), pp. 109-117
[14] Sun, J. L., *et al.*, Numerical and Experimental Investigation of Induction Heating Process of Heavy Cylinder, *Applied Thermal Engineering*, *134* (2018), Apr., pp. 341-352
[15] Bao, L., *et al.*, Numerical and Experimental Research on Localized Induction Heating Process for Hot Stamping Steel Sheets, *International Journal of Heat and Mass Transfer*, *151* (2020), Apr., 119422
[16] Zink, B., *et al.*, Thermal Analysis Based Method Development for Novel Rapid Tooling Applications, *International Communications in Heat and Mass Transfer*, *108* (2019), Nov., pp. 104297
[17] Jiang, S., *et al.*, Heating Properties of ERHCM Molds Based on Heating Cell Units, *Emerging Materials Research*, *8* (2019), 2, pp. 247-252
[18] Sanchez, R., *et al.*, Rapid Heating Injection Moulding: An Experimental Surface Temperature Study, *Polymer Testing*, *93* (2021), Jan., 106928
[19] Xu, Y., *et al.*, Numerical Simulation and Analysis of Phase Change Heat Transfer in Crude-Oil, *Thermal Science*, *25* (2021), 2A, pp. 1123-1134
[20] Xiao, C. L., Huang, H. X., Optimal Design of Heating System in Rapid Thermal Cycling Blow Mold by a Two-Step Method Based on Sequential Quadratic Programming, *International Communications in Heat and Mass Transfer*, *96* (2018), Aug., pp. 114-121
[21] Song, M. C., Moon, Y. H., Coupled Electromagnetic and Thermal Analysis of Induction Heating for the Forging Of Marine Crankshafts, *Applied Thermal Engineering*, *98* (2016), Apr., pp. 98-109
[22] Chen, S. C., *et al.*, Rapid Mold Temperature Variation for Assisting the Micro Injection of High Aspect Ratio Micro-Feature Parts Using Induction Heating Technology, *Journal of Micromechanics and Microengineering*, *16* (2006), 9, pp. 1783-1791
[23] Li, H. M., *et al.*, Numerical Simulations and Verifications of Cyclic and Transient Temperature Variations in Injection Molding Process, *Polymer-Plastics Technology and Engineering*, *48* (2008), 1, pp. 1-9
[24] Xiao, C. L., Huang H. X., Multiobjective Optimization Design of Heating System in Electric Heating Rapid Thermal Cycling Mold for Yielding High Gloss Parts, *Journal of Applied Polymer Science*, *131* (2014), 6, 39976
[25] Muszynski, P., *et al.*, Numerical Study of Rapid Cooling of Injection Molds, *Advances in Manufacturing Engineering and Materials*, Part of the Lecture Notes in Mechanical Engineering Book Series (LNME), 2019, pp. 539-547
[26] Ozcelik, B., Optimization of Injection Parameters for Mechanical Properties of Specimens with Weld Line of Polypropylene Using Taguchi Method, *International Communications in Heat and Mass Transfer*, *38* (2011), 8, pp. 1067-1072
[27] Fathi, S., Behravesh, A. H., Visualization of the Flow History Contours at the Cross-Section of a Weld-Line in an Injected Molded Part, *Journal of Applied Polymer Science*, *109* (2008), 1, pp. 412-417
[28] Liao, T., *et al.*, Predicting the Location of Weld Line in Microinjection-Molded Polyethylene Via Molecular Orientation Distribution, *Journal of Polymer Science Part B: Polymer Physics*, *57* (2019), 24, pp. 1705-171

Paper submitted: June 6, 2021
Paper revised: August 19, 2021
Paper accepted: August 27, 2021